On the incremental nonlinearity observed in a numerical model for granular media

Yuji Kishino

Summary

As a generalized constitutive relationship for granular media, incrementally nonlinear models have been proposed by many researchers. However, it is hard to evaluate the validity of such constitutive models in terms of experiments on real materials. On the other hand, the discrete element simulations have the capability to solve this problem. In this paper, true tri-axial stress-probe tests were simulated in terms of a discrete element method (Granular Element Method, or GEM). The result suggests that the exact behavior of granular media has to be described by a model with incremental nonlinearity. The stability in the incremental relationship between stress and strain is also discussed based on the second-order work.

1. Introduction

The so-called incrementally nonlinear constitutive models have been proposed and applied for the precise discussion on mechanical behavior of granular media [DARVE, 1984], [KOLYMBAS, 2000]. Such generalization of constitutive model seems to be crucial in the mechanics of granular media. However the choice of model obviously leads to different conclusions especially in such a study as the stability analysis of materials. Thus the evaluation of constitutive models should be made in a way or another.

A series of torsional shear tests on hollow cylindrical specimens of sand [PRADEL *et al.*, 1990] led the conclusion that, unlike the conventional flow rule, the direction of incremental plastic strain is dependent on the direction of incremental stress. The test results suggest that the incremental nonlinearity is inevitable for constitutive models of granular media. As the principal directions of incremental stress rotated in these tests, the incremental nonlinearity seemed to emerge from the rotation of principal axes of stress. On the other hand, the incremental nonlinearity under the loadings without rotation of principal axes has not yet been verified. A series of tri-axial tests [ANANDARAJAH *et al.*, 1995] showed the tendency that the flow behavior deviates from the classical flow rule. However, it seems rather hard to distinguish between the deviation from the theory and the fluctuation caused by specimens used in the tests. The rigorous evaluation of theories requires an accurate testing apparatus to perform multiple loadings and a lot of "identical" specimens for multiple loading paths. In real experiments, such requirements are hard to be cleared.

* Dept. of Civil Eng., Tohoku University, Sendai, Japan.

On the other hand, suitable discrete element approaches enable us to investigate diverse properties of an identical granular model, for we can carry out multiple loadings for an initial data or any other intermediate data. A series of numerical tests has been performed in terms of the Distinct Element Method to investigate the incremental response of granular media [BARDET, 1994]. The tests were restricted to 2D case and the accuracy of the control in stress probing was insufficient to extract a definite conclusion. Another discrete element method called the Granular Element Method [KISHINO, 1988] has been applied for the 3D study on the incremental response of granular media under the tri-axial stress states [KISHINO *et al.*, 2001]. The results showed that the Granular Element Method was effective for 3D stress-probe tests. However, the incremental nonlinearity was not so obvious to study. This paper, based on the true tri-axial tests, shows the definite nonlinearity in incremental response and discusses the stability given by the second-order work.

2. Method used for numerical tests

The simulation method used in this research is the 3D Granular Element Method (GEM), where the movement of each particle has 6 degrees of freedom: 3 components of parallel displacement and 3 components of rigid rotation. The incremental relationship between contact force and relative displacement at each contact point is characterized by stiffness coefficients in normal and tangential directions. Contact forces obey the Coulomb friction law and no-tension rule. According to these requirements, contact forces have to be modified time to time in an iterative procedure that leads to equilibrium configurations.

In the GEM algorithm, particle displacements and particle rotations in each iteration step are calculated by inverting individual stiffness matrices with 6 times 6 components assembled under the assumption that the neighboring particles do not move. This idea have stemmed from a relaxation method for the elastic frame analysis. However, the selection of relaxation procedure affects the results in non-elastic problems. In the relaxation procedure in GEM algorithm, the unbalanced forces and moments of particles are iteratively eliminated by moving particles according to their individual stiffness matrices, and actual particle movements in an iteration step take place at the same time for all of the particles only after their amounts are calculated thoroughly.

If a particle does not have at least three contact points, the stiffness matrix of this particle becomes singular. In the GEM algorithm, a singular stiffness matrix is replaced with a diagonal matrix whose components have small values. To avoid excess overlapping between particles, the particle movements calculated by the individual stiffness matrices are modified. Namely, the actual movements are determined by multiplying the calculated values by a common constant in such a way that the maximum movement does not exceed a limit.

The boundary shape of specimen used for numerical element tests can be arbitral. However, to avoid the direction-dependent behavior of the specimen, spheres may be preferable. Particles placed on the surface of a specimen are called peripheral particles and they are subjected to special movements by which the specimen is expected to deform homogeneously as a whole. When a material deforms homogeneously, the deformation field is expressed by a linear mapping of coordinates. When applying this restriction to the boundary, a peripheral particle transforms as follows:

$$\boldsymbol{x}^{\mathrm{P}} = \boldsymbol{T} \cdot \boldsymbol{X}^{\mathrm{P}} \qquad (1)$$

where $\boldsymbol{X}^{\mathrm{P}}$ and $\boldsymbol{x}^{\mathrm{P}}$ are the coordinates of the particle center in initial and current states and $\boldsymbol{T}$ is the deformation gradient. In element tests, we do not need to give the rigid rotation to the specimen and we assume $\boldsymbol{T}$ is symmetric. Then the compressive strain is defined by

$$\boldsymbol{\varepsilon} = -(\boldsymbol{T} - \boldsymbol{I}) \qquad (2)$$

where $\boldsymbol{I}$ is the unit tensor. By confining the rotations of peripheral particles, the number of independent variables required for the boundary control is 6 irrespective of the number of peripheral particles. In the relaxation procedure for strain-control tests, only thing required for the boundary control is to fix $\boldsymbol{T}$ until the relaxation process comes to an end. The role of peripheral particles, which may be looked upon as parts of a virtual testing device, is just to transmit boundary forces to an assembly of inner particles, and the interaction between peripheral particles, if any, is meaningless.

The resultant of contact forces applied to a peripheral particle P from inner particles is

$$\boldsymbol{F}^{\mathrm{P}} = \Sigma_C \boldsymbol{f}^{\mathrm{PC}} \qquad (3)$$

where $\boldsymbol{f}^{\mathrm{PC}}$ is a contact force at contact point C and Σ_C denotes the summation over the contact points. Then the Cauchy stress is defined as

$$\sigma = \frac{1}{V} \Sigma_{\mathrm{P}} \mathbf{x}^{\mathrm{P}} \mathbf{F}^{\mathrm{P}} \qquad (4)$$

where V is the current volume of the specimen and Σ_{P} denotes the summation over peripheral particles.

The stiffness relationship between σ and ε, under the assumption that the inner particles do not move, is easily determined by Equations (1) ~ (4) with the contact stiffness relationship. In the relaxation procedure for stress-control tests, the amount of incremental strain, which should be given repeatedly, is determined sufficiently by such a simplified stiffness relationship.

3. Numerical simulation of tri-axial test

The numerical specimen used in this research is shown in Fig. 1. The specimen is a random assemblage of 360 spherical particles whose radii range from 1.3 mm to 2.6 mm. Originally, it had just a geometrically admissible configuration and the cen-

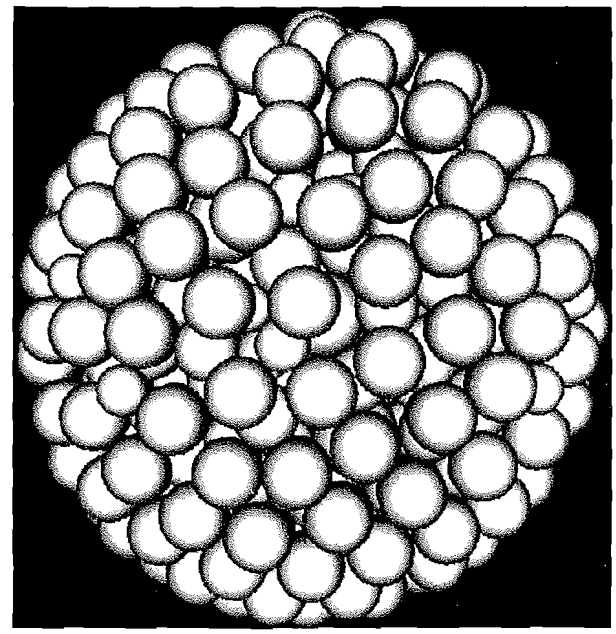

Fig. 1 – Numerical specimen.
Fig. 1 - Provino utilizzato nelle simulazioni numeriche.

Tab. 1 – Data used in numerical tests.
Tab. I – Parametri numerici.

Radius of smallest particle	1.3 mm
Radius of largest particle	2.6 mm
Number of particles	360
Number of peripheral particles	166
Spring constant for normal direction	2.0 MN/m
Spring constant for tangential direction	1.4 MN/m
Interparticle friction angle	15°
Initial confining pressure	0.1 MPa
Initial number of contact points	519
Norm of maximum displacement in a step	0.013 mm
Tolerance in boundary stress control	$\sqrt{3}\times10^{-7}$ MPa

ters of 166 peripheral particles were on a spherical surface. The initial configuration for numerical tests was obtained by isotropic compression by the 3D GEM code. The data used throughout in this paper are listed in Tab. I. A very small magnitude for the tolerance in the boundary stress control is chosen because we need to calculate both the elastic and plastic strains accurately. Such an accurate stress control could not be achieved without adopting a stiffness method as in GEM. Several other specimens with different numbers of particles were also utilized to investigate mechanical responses of granular material elements. The results, that are not shown in this paper, exhibit smooth responses even for a specimen with the fewer number of particles. Thus it can be said that the number of particles is sufficient to know global behaviors as a material element. It should be noted that we will need far more particles to investigate general boundary-value-problems.

At first, a tri-axial compression test was carried out. In the test, the only stress component changed was the axial stress σ_z and the other stress components were kept constant: $\sigma_x = \sigma_y = p_0$ and $\tau_{yz}=\tau_{zx}=\tau_{xy}=0$. Fig. 2 shows the calculated results for 6 strain components in the tri-axial compression test. The stress ratio in this figure is the ratio between the absolute value of stress deviator and the mean stress. In the range where the stress ratio is far below its peak value, the two lateral strain components ε_x and ε_y are almost identical, and the shear strain components ε_{yz}, ε_{zx} and ε_{xy} are almost zero, which means that the principal directions of stress and strain tensors almost coincide with each other. As σ_z increases, ε_{yz}, ε_{zx} and ε_{xy} as well as ε_x–ε_y increase gradually, which suggests that the unsymmetrical anisotropy develops in the specimen.

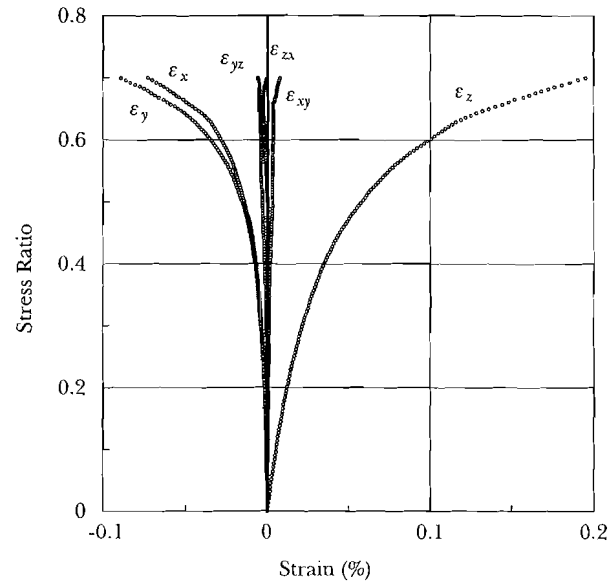

Stress Ratio = absolute value of stress deviator / mean stress

Fig. 2 – Stress-strain relationship.
Fig. 2 – Curva sforzo-deformazione (compressione triassiale).

4. Numerical simulation of stress-probe tests

A series of numerical stress-probe tests was carried out, starting from an intermediate data obtained by the tri-axial compression test explained in the previous section. As shown in Fig. 3, a stress-probe test is a set of incremental loading and reversal loading along a specified stress-probe direction, which gives the incremental elastic strain as the recoverable part and the incremental plastic strain as the irrecoverable part.

All of the stress-probe directions in this paper lie in the principal stress space, and the stress-probe tests in 72 directions on a plane form a series of probe tests. The magnitude of each stress-probe was $|d\sigma| = 0.001$ MPa which is one hundredth of the initial confining pressure p_0. The starting data of stress-probe tests was the output data obtained by the tri-axial compression test at the stress ratio 0.4. The stress-probe directions are represented by the angles from the inward normal of the yield surface.

Fig. 4 shows two types of probe tests carried out in this paper. To specify probe directions, we define three characteristic directions based on a yield surface. We assume that the yield surface is a cone whose vertex is at the origin of the principal stress space. The validity of this assumption, at least in the vicinity of the current stress point for tri-axial loading, will be verified by the results shown later. We will also find later that we cannot assume the existence of a smooth yield surface for general incremental stresses. However, we define characteristic directions by assuming that the yield surface is the

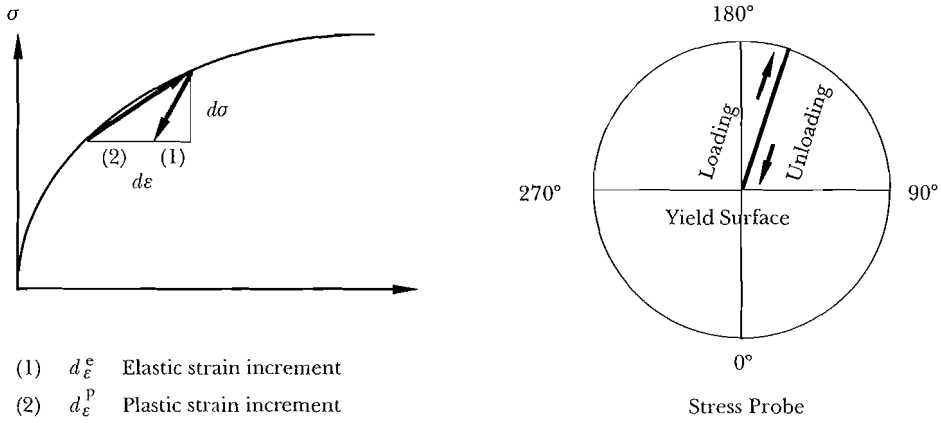

Fig. 3 – Stress-probe test.
Fig. 3 – Descrizione dei percorsi di carico incrementale.

cone explained above. In the principal stress space, σ is a generator of the yield surface and its direction

$$\mathbf{l} = \frac{\sigma}{|\sigma|} \tag{5}$$

is the first characteristic direction. The second characteristic direction is the outward normal of the yield surface, which, by assuming symmetric mechanical properties with respect to x and y directions, is given by

$$\mathbf{n} = \frac{\sigma - \sigma_0 - (\sigma - \sigma_0) : \mathbf{l}\,\mathbf{l}}{|\sigma - \sigma_0 - (\sigma - \sigma_0) : \mathbf{l}\,\mathbf{l}|} \tag{6}$$

where σ_0 is the initial isotropic stress in the tri-axial compression test. The third characteristic direction $\boldsymbol{m}$ is perpendicular to these directions as shown in Fig. 4.

The probe planes for Probe Test 1 and Probe Test 2 are planes specified by combinations of direction vectors as (n, l) and (n, m) respectively. In Probe Test 1, all of the stress-probes satisfy $d\sigma_x = d\sigma_y$ and the stress state always remains in the so-called tri-axial state, while, in Probe Test 2, the stress state is generally in the so-called true tri-axial state.

Figs. 5 and 6 show the incremental strains obtained in the stress-probe tests. Stress-probes and incremental strains are plotted in the principal stress space and the relevant principal strain space. The principal directions of incremental strains are not generally the same as those of stress. However, judging from Fig. 2, we may assume that the differences are very small. As for the incremental elastic re-

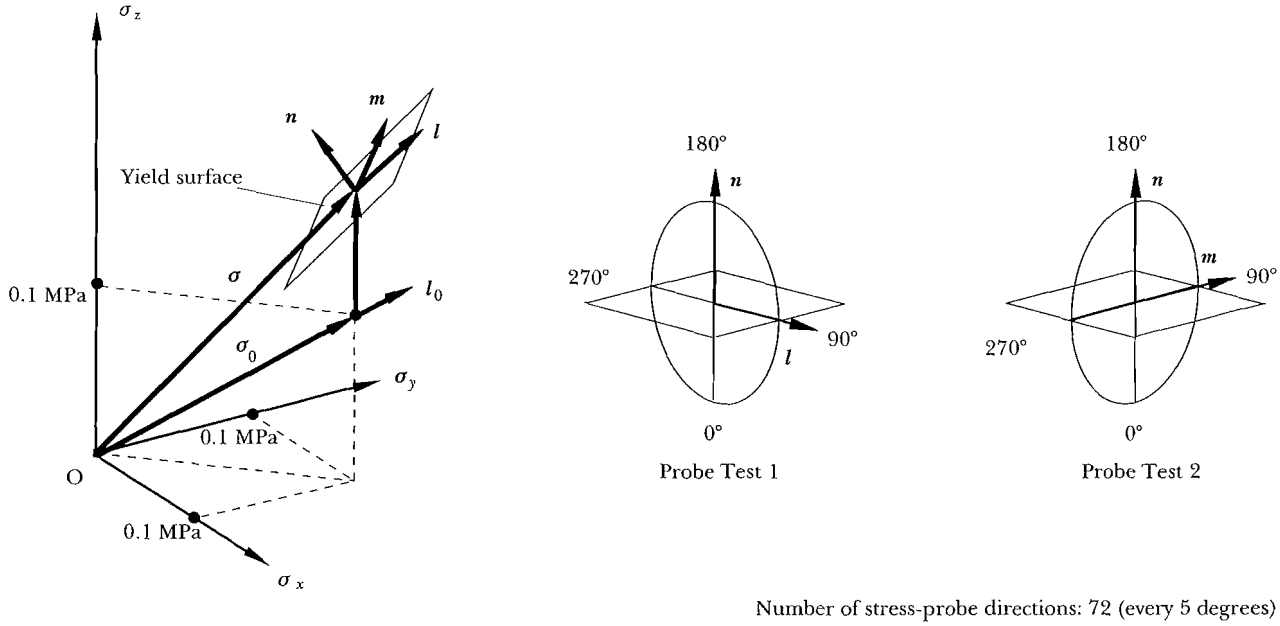

Fig. 4 – Stress-probe directions.
Fig. 4 – Direzione dei percorsi di carico incrementale.

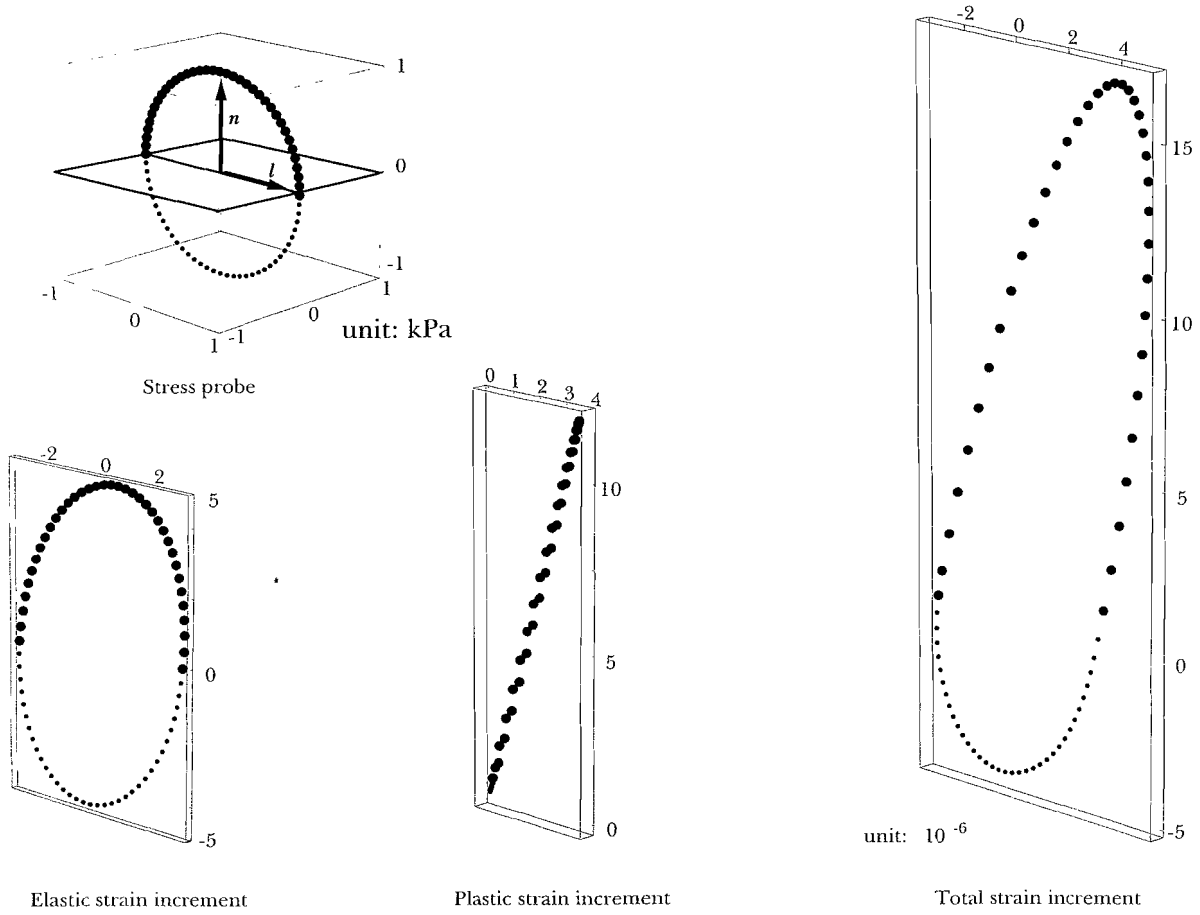

Fig. 5 – Incremental response (Probe Test 1).
Fig. 5 – Risposta incrementale (Probe Test 1).

sponse, we can predict the results in terms of the generalized Hooke's law with slight anisotropy.

The incremental response for a stress-probe that has downward normal component with respect to the yield surface is usually assumed to be elastic, and in fact the incremental plastic strains in Probe Test 1 are almost zero as shown by gray colored plots. The result is also in accord with the previous assumption that the yield surface is given by a cone whose vertex is at the origin of the principal stress space. Further, in Probe Test 1, it is observed that the incremental plastic strain vectors are almost on a straight line. As the straight line is not coaxial with the outward normal of yield surface, the plastic flow is non-associative.

On the other hand, the incremental plastic response in Probe Test 2 is totally different from the above result (Fig. 6). The incremental plastic strain vectors are not on a unique straight line and the direction of incremental plastic strain is apparently dependent on the direction of incremental stress. Further, the gray plots that represent incremental plastic strains for stress-probes that have downward normal components with respect to the yield surface indicate that the assumption of the existence of flat yield surface does not hold.

To investigate the plastic behavior thoroughly, the amounts of incremental plastic strains are plotted against the stress-probe directions defined in Fig. 4. The plots are shown in Fig. 7. The components of incremental plastic strains in this figure are the projected values on three characteristic directions. In the result of Probe Test 1, the plastic strain emerges for the stress-probe directions from 90 to 270 degrees. If the plastic flow obeys the associated flow rule, the only non-zero component should be $d\varepsilon^p_n$. However we also have $d\varepsilon^p_l$ that could not be discarded and $d\varepsilon^p_m$ whose value is comparatively negligible. The last component stems from the mechanical anisotropy of the specimen used in this paper. These curves in the plastic range are almost fitted into half cycles of sinusoidal curves except for incremental plastic strains with very small values, which means that the incremental plastic strain is almost proportional to the projection of incremental stress onto the outward normal of yield surface: $\boldsymbol{n}:d\sigma$. Thus, as far as Probe Test 1 concerns, the plastic flow may be predicted approximately by the non-associated flow rule.

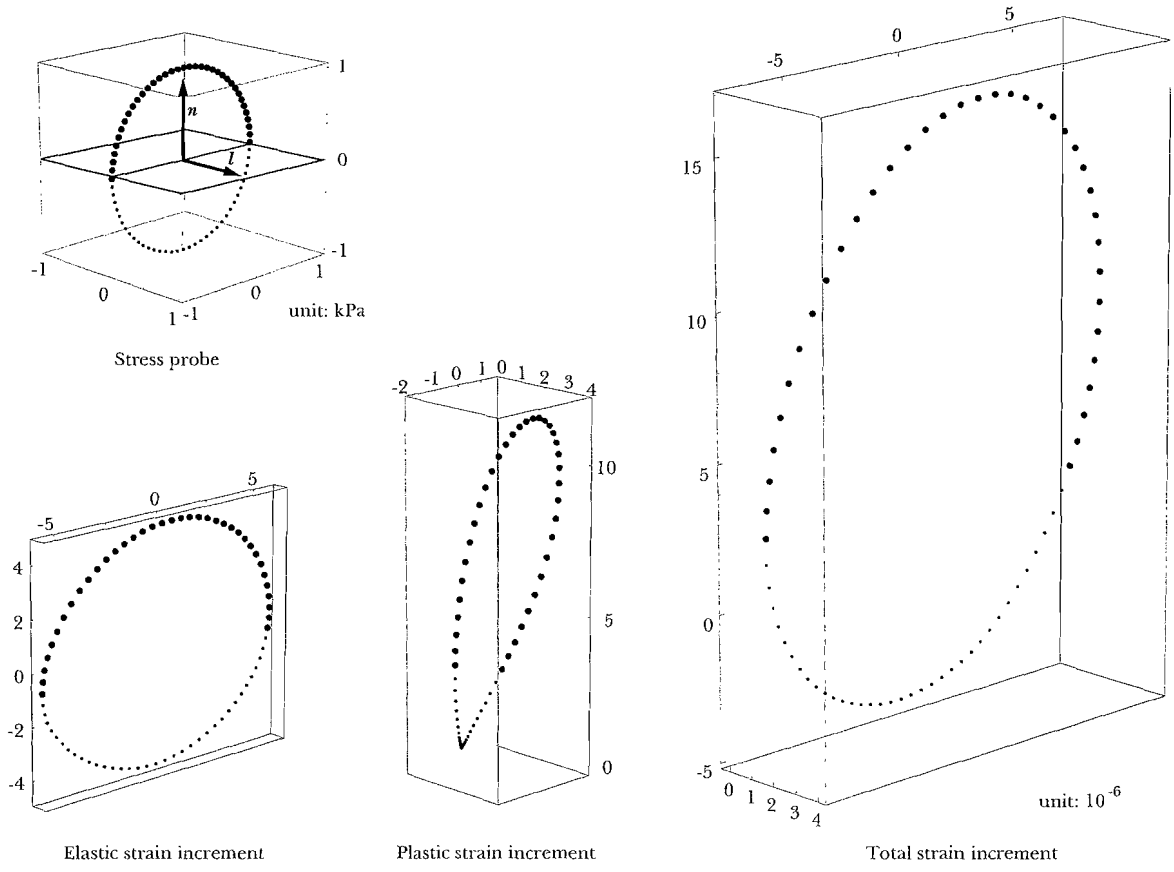

Fig. 6 – Incremental response (Probe Test 2).
Fig. 6 – Risposta incrementale (Probe Test 2).

Observing the result of Probe Test 2, we notice first that the plastic range spreads beyond the region from 90 to 270 degrees, which means that we could not assume a flat yield surface. Further the change in $d\varepsilon^p{}_m$ is by no means proportional to $\boldsymbol{n}:d\boldsymbol{\sigma}$ Instead, it is synchronizing with the tangential component of incremental stress $\boldsymbol{m}:d\boldsymbol{\sigma}$. From these results, we may conclude that the plastic deformation is accompanied by multiple shear mechanisms. One of the definite mechanisms is that of tri-axial shearing which has been developing during the tri-axial compression. Another mechanism begins to develop when the specimen experiences the shearing $d\sigma_x$–$d\sigma_y$ for the first time in Probe Test 2. By admitting the existence of multiple shear mechanisms, we can easily understand the incremental plastic response that depends on $\boldsymbol{m}:d\boldsymbol{\sigma}$ in Probe Test 2. Another series of stress-probe tests has been carried out to simulate the torsional shear tests [PRADEL *et al.*, 1990] and the result exhibits the incremental nonlinearity just in the same way as in the real tests.

From these observations, it is concluded that the real behavior of granular media inevitably includes the incremental nonlinearity that is caused by multiple shear mechanisms in plastic deformation.

5. Plastic flow model

In this section, we will discuss the primitive plastic flow model that can predict the incremental plastic response obtained in the previous section. Here we assume that the principal directions of incremental stress and incremental plastic strain coincide. Let us decompose the stress rate into the three characteristic directions stated in the previous section as follows:

$$\dot{\boldsymbol{\sigma}} = (N\boldsymbol{n} + L\boldsymbol{l} + M\boldsymbol{m}) \mid \dot{\boldsymbol{\sigma}} \mid \tag{7}$$

where

$$N = \boldsymbol{n}:\boldsymbol{t} \quad L = \boldsymbol{l}:\boldsymbol{t} \quad M = \boldsymbol{m}:\boldsymbol{t} \tag{8}$$

are the normalized components in the characteristic directions, and

$$\boldsymbol{t} = \dot{\boldsymbol{\sigma}} \mid \dot{\boldsymbol{\sigma}} \tag{9}$$

denotes the direction of stress rate. Corresponding to this decomposition of stress rate, we decompose the plastic strain rate as follows:

$$\dot{\boldsymbol{\varepsilon}}^p = \{f(N,L,M)\boldsymbol{n} + g(N,L,M)\boldsymbol{l} + h(N,L,M)\boldsymbol{m}\}|\dot{\boldsymbol{\sigma}}| \tag{10}$$

where f, g and h are functions of N, L and M. In the conventional plastic model as well as the model with

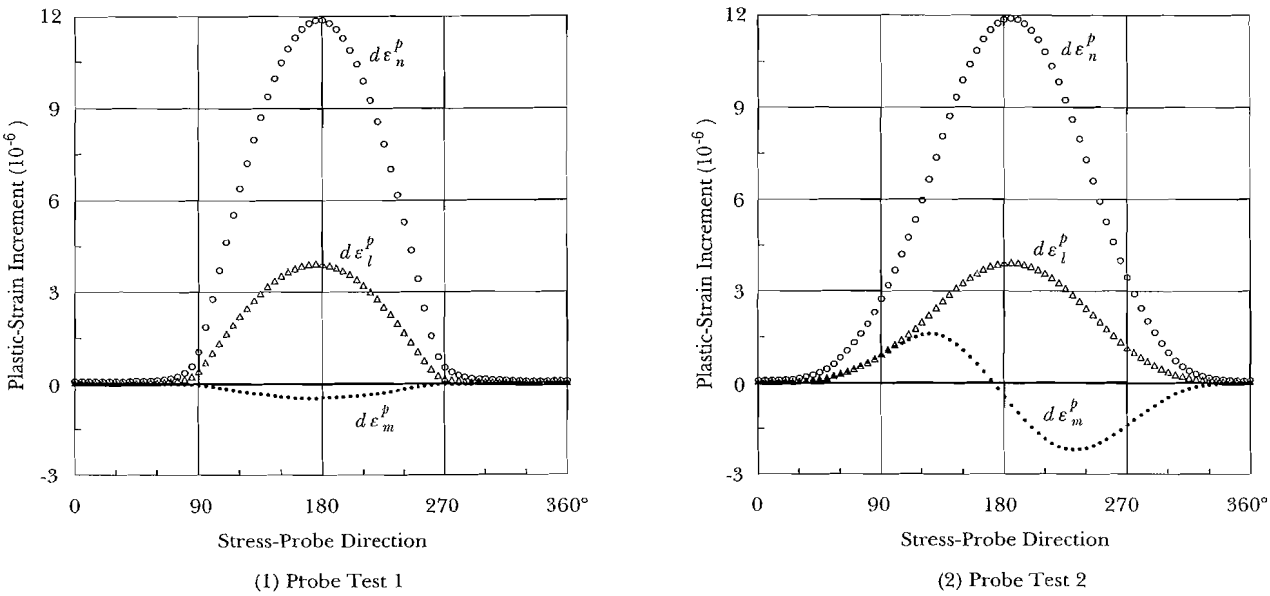

Fig. 7 – Incremental plastic strain obtained in stress-probe test.
Fig. 7 – Deformazioni incrementali plastiche determinate numericamente.

the so-called tangential stress rate effect [HASHIGUCHI *et al.*, 2001], the above functions are expressed by linear functions in each of the elastic and plastic regions. However, the results for Probe Test 1 and Probe Test 2 obtained in the previous section never fit any combination of linear functions. Instead, we have to assume such a nonlinear function as follows:

$$f(N,L,M)=\frac{1}{\eta}\left(\frac{1}{2}N+\frac{1}{2}\sqrt{\frac{1.01L^2}{1-N^2}-L^2}+\frac{1}{2}\frac{M^2}{1-N^2}-\frac{1}{4}M^2\right) \quad (11)$$

$$\begin{aligned} g(N,L,M) &= a\cdot f(N,L,M) \\ h(N,L,M) &= bMf\cdot(N,L,M) \end{aligned} \quad (12)$$

where η is a hardening parameter and a and b are proportional factors. Fig. 8 shows the incremental plastic response calculated according to the above model with assumed constants: $a=0.33$ and $b=0.28$. The magnitudes of incremental plastic strains are normalized by the maximum value of $d\varepsilon^p{}_n$. The plots with a sign "A.F.R." show the values of $d\varepsilon^p{}_n$ predicted by the associated flow rule. As shown in Fig. 8, the incremental plastic strains predicted by the proposed model are in good agreement with the result of numerical tests given in Fig. 7. Equation (10) is a continuous function for all the stress-probe directions and we do not need to prepare the different functions for elastic and plastic regions. However, the equation has the more complicated form compared with the 2nd order nonlinear model [DARVE, 1984]. The more complicated form may be needed to incorporate such an incremental stress that causes the rotation of principal axes of stress.

6. Second order works

The stability in the incremental relationship between stress and strain were investigated by calculating the total and plastic second-order works: $d^2w=d\sigma:d\varepsilon$ and $d^2w^p=d\sigma:d\varepsilon^p$. Figs. 9 and 10 show the second-order works in the stress-probe tests stated above, as well as in other probe tests carried out at the stress ratio 0.6. As is observed in these figures, the total second-order work d^2w is always positive and Hill's stability condition [HILL, 1958] is satisfied for all the stress-probes. The smallest value of d^2w is found in Probe Test 1 for a stress-probe whose direction is close to the tangential direction of yield surface. The plastic second-order work d^2w^p takes slightly negative values for stress-probe directions where the incremental plastic strain takes small values, which means that the Drucker's postulate [DRUCKER, 1959] is violated in some extent. Irrespective of the negative values of d^2w^p, the incremental plastic strains were calculated stably for all the stress-probes.

In the stress-probe tests at the stress ratio 0.6, d^2w is positive but the difference between second-order works $d^2w-d^2w^p$ tends to be smaller. The stress ratio 0.6 is still far below the peak value and it is possible that d^2w becomes negative for a certain stress-probe before the stress-strain curve reaches the peak point. Such an instability condition will be investigated in future numerical tests. However, it can be predicted from Fig. 6 that the unstable direction, if any at least for the monotonic tri-axial loading, is given by the incremental stress tensor whose direction in the principal stress space is very close to the direction of $-\sigma$ or σ.

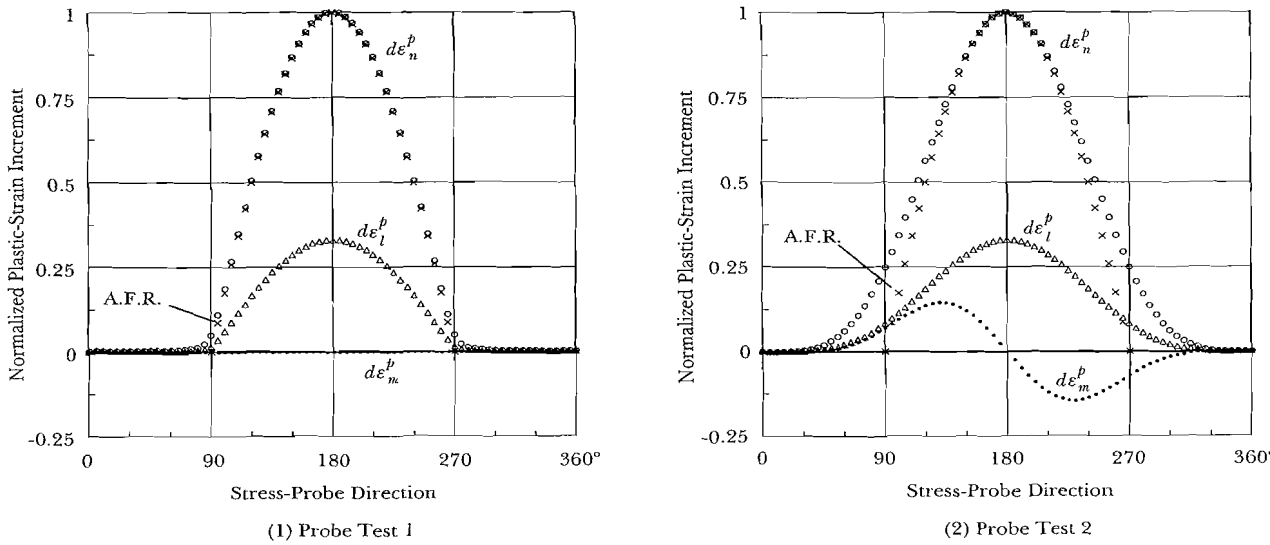

Fig. 8 – Incremental plastic strain given by Equation (10).
Fig. 8 – Deformazioni incrementali plastiche secondo l'Equazione (10).

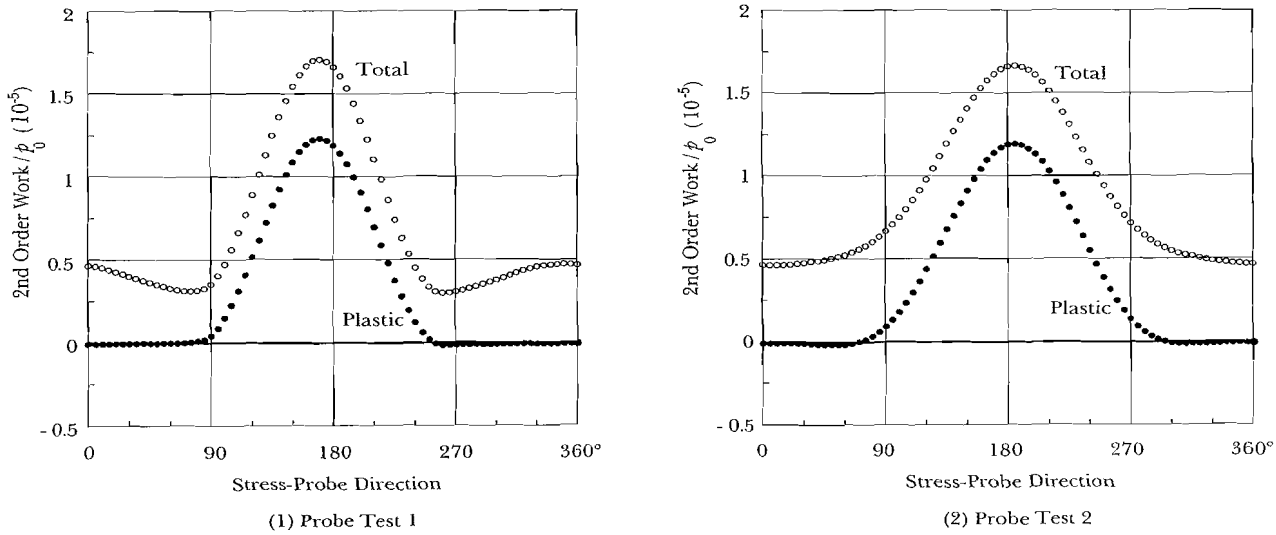

Fig. 9 – 2nd order work (stress ratio: 0.4).
Fig. 9 – Lavoro del second'ordine (livello di carico iniziale: 0.4).

7. Conclusion

In this paper, the numerical tests were carried out to verify the incremental nonlinearity in constitutive relationship for granular media. The method used was the 3D Granular Element Method, and the simulation of true tri-axial probe tests led to the following results:

1) As far as the simulation of conventional tri-axial stress-probe test concerns, the incremental plastic response seems to be approximated by the non-associated flow rule.
2) For general stress-probes in true tri-axial state, the direction of incremental plastic strain is apparently dependent on the direction of incremental stress.
3) The flat yield surface cannot be assumed, which suggests the existence of multiple shear mechanisms in plastic deformation.
4) An incrementally nonlinear model derived through the decomposition of incremental stress in three characteristic directions can predict the incremental plastic response in true tri-axial state.
5) The Hill's condition of stability is satisfied for all the stress-probes in this paper, while the Drucker's condition of stability is not satisfied for some stress-probe directions.
6) The unstable stress-probe direction, if any at least for the monotonic tri-axial loading, will be very close to the direction of $-\sigma$ or σ.

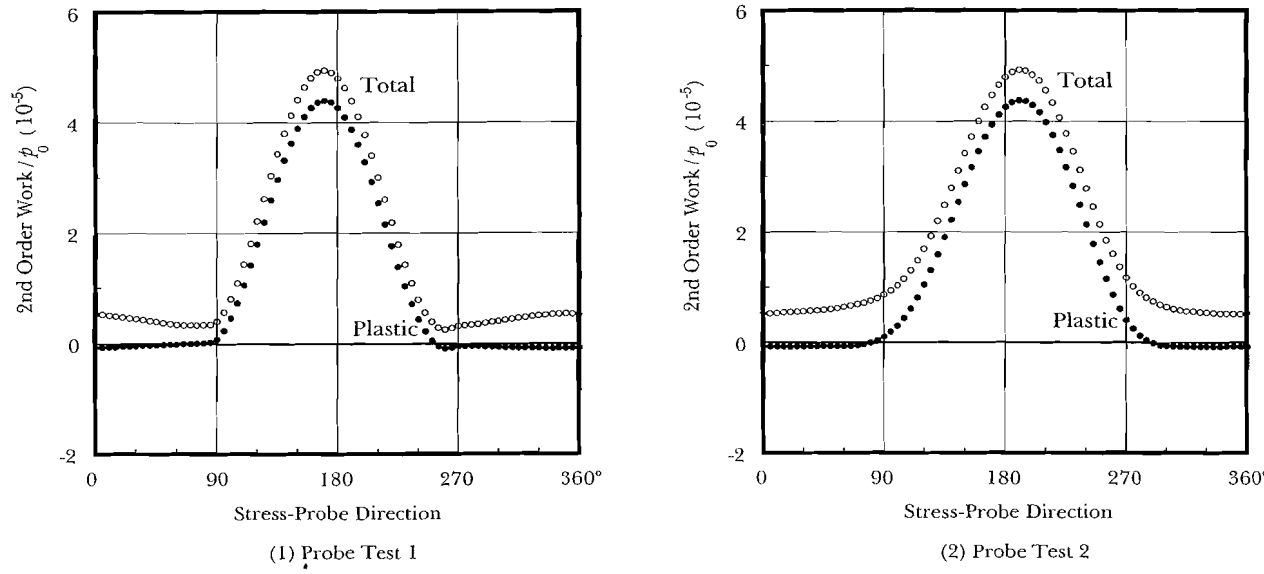

Fig. 10 – 2nd order work (stress ratio: 0.6).
Fig. 10 - Lavoro del second'ordine (livello di carico iniziale: 0.6).

References

ANANDARAJAH A., KHALED S., KUGANENTHIRA N. (1995) – *Incremental Stress-Strain Behavior of Granular Soil.* ASCE Journal of Geotechnical Engineering, 121(1), pp. 57-67.

BARDET J.P. (1994) – *Numerical Simulations of the Incremental Responses of Idealized Granular Materials.* International Journal of Plasticity, 10(8), pp. 879-908.

DARVE F. (1984) – *An Incrementally Non-Linear Constitutive Law: Assumptions and Predictions.* in *Constitutive Relations for Soils* (eds., G. Gudehus, F. Darve & I. Vardoulakis), A.A. Balkema, pp. 385-403.

DRUCKER D.C. (1959) – *A Definition of Stable Inelastic Material.* Journal of Applied Mechanics, 26, pp. 101-106.

HASHIGUCHI K., TSUTUSMI S. (2001) – *Elastoplastic constitutive equation with tangential stress rate effect*, Int. Jour. Plasticity, 17, pp. 117-145.

HILL R. (1958) – *A General Theory of Uniqueness and Stability in Elastic-Plastic Solids.* Journal of the Mechanics and Physics of Solids, 6, pp. 236-249.

KISHINO Y. (1988) – *Disc Model Analysis of Granular Media. Micromechanics of Granular Materials* (eds., M. Satake & J.T. Jenkins), Elsevier, pp. 143-152.

KISHINO Y., AKAIZAWA H., KANEKO K. (2001) – *On the Plastic Flow of Granular Materials.* in *Powders & Grains 2001* (ed., Y. Kishino), A.A. Balkema, pp. 199-202.

KOLYMBAS D. (Editor) (2000) – *Constitutive Modelling of Granular Materials.* Springer, Berlin.

PRADEL D., ISHIHARA K., GUTIERREZ M. (1990) – *Yielding and Flow of Sand under Principal Stress Axes Rotation.* Soils and Foundations, 30(1), pp. 87-99.

Studio tramite modello numerico della non linearità incrementale dei materiali granulari

Sommario

Modelli costitutivi incrementalmente non-lineari di vario genere sono stati proposti da molti ricercatori per interpretare il comportamento meccanico dei materiali granulari. La via sperimentale per la conferma della validità di tali modelli è irta di difficoltà. D'altro canto, l'uso di simulazioni numeriche discrete è in grado di risolvere molti dei problemi legati all'approccio sperimentale. In questo articolo, un particolare modello numerico discreto (Granular Element Method, GEM) viene utilizzato per simulare la risposta di un materiale granulare idealizzato sottoposto ad una serie di sollecitazioni incrementali, in condizioni triassiali "vere". I risultati indicano che il comportamento osservato può essere convenientemente descritto da un modello incrementalmente non-lineare. Inoltre, la stabilità della relazione costitutiva incrementale è discussa sulla base delle misure effettuate in termini di lavoro del second'ordine.